
Analysis and instrumentation for a xenon-doped liquid argon system

Ryan Gibbons

Work completed under the advisement of Professor Michael Gold

Department of Physics and Astronomy
The University of New Mexico

May 27, 2020

Abstract

Liquid argon is a scintillator frequently used in neutrino and dark matter experiments. In particular, is the upcoming LEGEND experiment, a neutrinoless double beta decay search, which will utilize liquid argon as an active veto system. Neutrinoless double beta decay is a theorized lepton number violating process that is only possible if neutrinos are Majorana in nature. To achieve the LEGEND background goal, the liquid argon veto must be more efficient. Past studies have shown the addition of xenon in quantities of parts-per-million in liquid argon improves the light yield, and therefore efficiency, of such a system. Further work, however, is needed to fully understand the effects of this xenon doping. I present a physical model for the light intensity of xenon-doped liquid argon. This model is fitted to data from various xenon concentrations from BACoN, a liquid argon test stand. Additionally, I present preliminary work on the instrumentation of silicon photomultipliers for BACoN.

Contents

1	Introduction	4
1.1	Neutrinos and double beta decay	4
1.2	LEGEND and BACoN	5
1.3	Liquid argon	6
2	Physical modeling of xenon-doped liquid argon	8
2.1	Model	8
2.2	Fits to BACoN Data	9
2.3	Analysis of Rate Constant	12
3	Instrumentation of SiPMs	12
4	Conclusions and Future Work	13

1 Introduction

1.1 Neutrinos and double beta decay

Neutrinos are neutral leptons that come in three flavors: electron, muon, and tau. Unlike the other fundamental particles, neutrinos of a certain flavor are a combination of oscillating mass states and, as a result, neutrinos oscillate between flavors. The discovery of neutrino oscillations conflicts with the current Standard Model of Particle Physics, and indeed requires the introduction of new physics [1, 2].

A promising theory beyond the Standard Model is neutrinos being Majorana fermions. When developing solutions of the Dirac equation, two methods, Dirac and Majorana, can be utilized. The familiar Dirac method involves a four-component spinor, implying the existence of a particle's antiparticle [2]. Fermions other than neutrinos are successfully described this way. The Majorana method, on the other hand, involves only a two-component spinor, implying no distinction between a particle and its antiparticle [2]. In other words, a Majorana fermion is its own antiparticle. An immediate requirement of a Majorana fermion is it must be neutral, as it remains unchanged by charge conjugation. Hence, as neutrinos are the only neutral fundamental fermions, they are the only candidates to be Majorana fermions [2, 3]. Although it is unknown if neutrinos are Dirac or Majorana, many extensions of the Standard Model, including 'seesaw' neutrino mass mechanisms, predict Majorana neutrinos. Additionally, in a physical view, Majorana neutrinos give way to processes that violate lepton number conservation. This entails the creation of more matter than antimatter and vice versa. Majorana neutrinos then support theories of leptogenesis, which provide answers to the observed asymmetry of matter and antimatter in the universe [2, 1].

The only known way to confirm the existence of Majorana neutrinos is by observing the lepton number violating nuclear process, neutrinoless double beta decay ($0\nu\beta\beta$) [3]. Understanding $0\nu\beta\beta$ first requires understanding normal, or neutrino-full, double beta decay ($\beta\beta$). This well-known process is when a parent nucleus, with mass (nucleon) number A and atomic number Z , decays into a daughter nucleus of the same A , with atomic number $Z + 2$. Nuclei decay in this fashion when the binding energy of the daughter nucleus from single beta decay is greater than the parent, in which case single beta decay energetically forbidden, but the binding energy of the daughter nucleus from $\beta\beta$ is less than the parent [3]. Along with the change of the nucleus, in $\beta\beta$, two electrons and neutrinos are produced:

$$(A, Z) \rightarrow (A, Z + 2) + 2e^- + 2\bar{\nu}_e \quad (1)$$

If neutrinos are Majorana fermions, then these two neutrinos can be exchanged as virtual particles, and the electrons gain the energy of the neutrinos, giving us $0\nu\beta\beta$:

$$(A, Z) \rightarrow (A, Z + 2) + 2e^- \quad (2)$$

In detecting any double beta decay, the relevant measurement is the sum of the two electron energies. In the case of $\beta\beta$, the decay is described with two body kinematics between the electrons and neutrinos. For $0\nu\beta\beta$, the decay is described by the single body kinematics of the two electrons. The expected energy spectrum of $0\nu\beta\beta$ is then a sharp peak slightly greater than $Q_{\beta\beta}$, the largest amount of energy given to the electrons in $\beta\beta$ decay. Figure 1 shows a plot of the energy distribution of the two electrons from the preceding discussion [1].

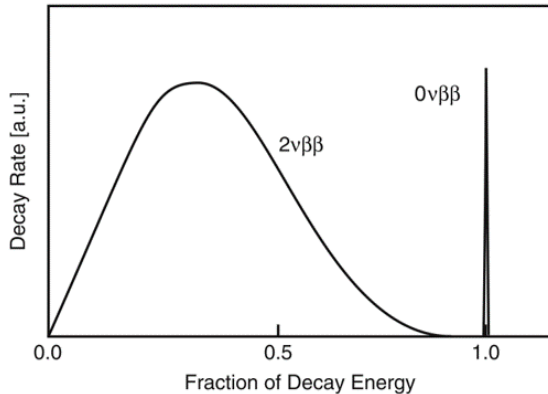


Figure 1: Summed electron energy spectrum of double beta decays. Note the height of the $0\nu\beta\beta$ peak is exaggerated for clarity [1].

1.2 LEGEND and BACoN

The central experimental challenge in detecting $0\nu\beta\beta$ is the exceptionally long half-lives. $\beta\beta$ is known to have half-lives of the order 10^{21} years, and $0\nu\beta\beta$ is theorized to have half-lives of order 10^{28} [3]. As such, experimental efforts focus on scaling detectors to large sizes and eliminating background events. One such planned experiment is the Large Enriched Germanium Experiment for Neutrinoless double beta Decay (LEGEND). LEGEND plans to use 1 ton of enriched germanium as a source and detector, surrounded by liquid argon [4]. Liquid argon will cool the germanium, producing less thermal noise, and also act as a background rejection system, known as an active veto. This is possible due to LAr being a scintillating material, that is, it produces light from the passage of ionizing radiation. When a background radiation event enters the experiment, it will pass through the LAr and germanium. By detecting these events in coincidence, these extraneous events are vetoed from the data.

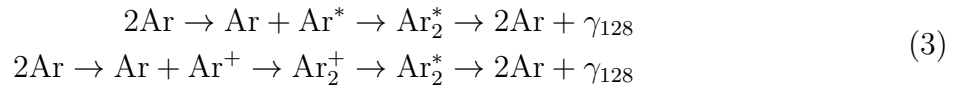
The LEGEND background goal is < 0.1 events/(FWHM-ton-year) in the region of interest [4]. That is to say, in the energy bins of interest, given one ton of germanium and one year of run time, we expect 0.1 background events. This is the most ambitious background goal by a $0\nu\beta\beta$ experiment, and currently, the best germanium-LAr background is about 1 events/(FWHM-ton-year) by the GERDA-II experiment [3]. Significant efforts in improving the LAr active veto are then needed to reach the LEGEND goal. To improve the LAr veto, one needs a higher detection efficiency, which is dictated by the light yield. Essentially, one wants to collect the maximum amount of light from scintillation events. There are several efforts to improve the LAr veto in LEGEND, including an experiment known as BACoN.

BACoN is a 100 liter LAr system at the University of New Mexico. It serves as a test stand for investigating ways of improving the liquid argon veto in LEGEND. Of current interest to BACoN are the effects of adding parts-per-million (ppm) amounts of fluids to the LAr, known as doping the LAr, with xenon being in particular interest. To collect LAr scintillation, two Hamamatsu R11065 photomultiplier tubes (PMTs) are used. Additionally, two acrylic disks coated with tetraphenyl butadiene (TPB) are attached above the PMT windows, the significance of which will be explained in a further section. Recent results from

BACoN show that by adding 10 ppm of xenon, one measures an increase in the light yield of factor 1.8. Further work with xenon doping is expected, and as such, significant hardware upgrades are also in progress.

1.3 Liquid argon

The process of liquid argon scintillation is understood by the following: ionizing radiation enters liquid argon, then either ionizes or excites argon atoms. These altered atoms then form an excited argon dimer, which then deexcites by emitting 128 nm light, which is in the vacuum ultra violet range (VUV). This process is described by [5]:



The excited dimers can be in either a singlet, $s = 0$, or triplet, $s = 1$, quantum state. In both cases, the deexcitation is exponential with a lifetime. The singlet lifetime is $\tau_s = 7$ ns, while the triplet lifetime is $\tau_t = 1.8 \mu\text{s}$ [5]. The resulting change in the number of excimer states can be modeled by a simple exponential:

$$\begin{aligned} \frac{dS(t)}{dt} &= -\frac{1}{\tau_s} S(t) \rightarrow S(t) = S_0 e^{-t/\tau_s} \\ \frac{dT(t)}{dt} &= -\frac{1}{\tau_t} T(t) \rightarrow T(t) = T_0 e^{-t/\tau_t} \end{aligned} \quad (4)$$

Here, S_0 and T_0 are the initial concentrations of singlet and triplet states respectively. The ratio of singlet and triplet light is dependant on the type of radiation that causes the scintillation event. This is the subject of pulse shape discrimination, which is used to determine the source of an event based on the light intensity. The light intensity is the sum of change in the number of states due to scintillation:

$$L(t) = \frac{S_0}{\tau_s} e^{-t/\tau_s} + \frac{T_0}{\tau_t} e^{-t/\tau_t} \quad (5)$$

In addition to the liquid scintillation, if there exists a gaseous ullage, then the argon gas scintillation must be taken into account. The singlet lifetime in gaseous argon is comparable to the singlet lifetime in liquid, and as such the gaseous singlet light can be included in the liquid singlet state. The gaseous triplet lifetime has a value of $\tau_g = 3.5 \mu\text{s}$ [6], and as such an additional term must be added to Equation 5:

$$L(t) = \frac{S_0}{\tau_s} e^{-t/\tau_s} + \frac{T_0}{\tau_t} e^{-t/\tau_t} + \frac{G_0}{\tau_g} e^{-t/\tau_g} \quad (6)$$

The measured light intensity in liquid argon is altered by several factors. First, the design of the experiment is crucial in ensuring there are no spacial blind spots in detection. Second, the purity of liquid argon. Contaminants such as oxygen and nitrogen can significantly alter the light yield, in concentrations as little as 5 ppm [7]. This happens due to excited argon dimers colliding with contaminants, transferring energy before the argon gives off light.

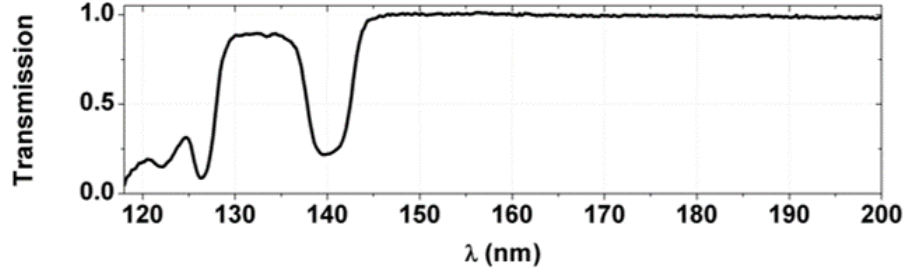


Figure 2: LAr transparency as a function of wavelength. At 128 nm, LAr has about 50% transparency, where as longer wavelengths give values closer to 100% [5].

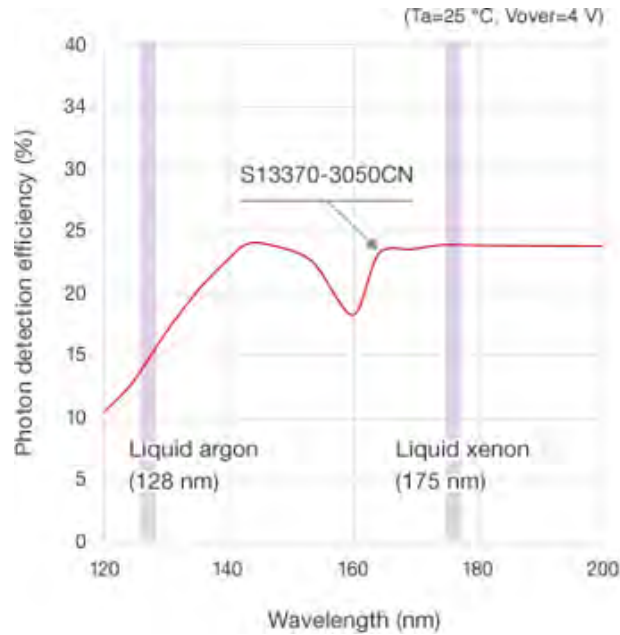


Figure 3: The photodetection efficiency of a SiPM vs wavelength. This particular model, Hamamatsu S13370-3050CN, is specifically designed for use in the VUV range. The higher wavelengths are shown to have better efficiency.

Third, the wavelength of light. Argon scintillates at 128 nm; however, longer wavelengths are advantageous as LAr becomes more transparent, and photodetectors are generally more efficient [5, 8].

Current and past experiments have used TPB as a method of wavelength shifting. TPB will absorb 128 nm light, and reemit light at 430 nm. The general procedure has been to have a thin layer of TPB situated above the window of a photodetector. While this improves the light yield, the LAr transparency issue remains. Additionally, TPB reemits light isotropically, leading to at least a 50% drop in potential light yield.

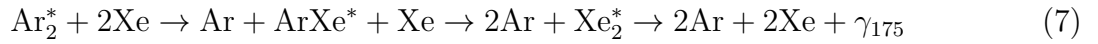
A proposed alternative to TPB is xenon doping: the insertion of xenon on the order of ppm into LAr. This shifts the wavelength of light to the xenon scintillation wavelength of 175 nm through a transfer in energy from the diffusion of the excited LAr dimers [8]. This then addresses both the LAr transparency and photodetector efficiency issues. Indeed, past

studies have shown an increase in light yield from xenon doping [5, 8].

2 Physical modeling of xenon-doped liquid argon

2.1 Model

As mentioned previously, the model for xenon-doped LAr is through a transfer in energy through collisions. The excited argon dimers can either deexcite emitting a photon or collide with xenon atoms to form an argon-xenon mixed excited state. This mixed state then collides with other xenon atoms, forming excited xenon dimers, which then deexcite, emitting a photon at 175 nm. This process is written as [8]:



To quantify the light output from this process, we consider the number of states in each type:

- $S(t)$ the argon excimer singlet state
- $T(t)$ the liquid argon excimer triplet state
- $G(t)$ the gaseous argon excimer triplet state
- $M(t)$ the argon-xenon mixed state
- $X(t)$ the xenon excimer triplet state

Through the transfer process described previously, the following set of equations describe the change in these states:

$$\begin{aligned} \frac{dS(t)}{dt} &= -\frac{1}{\tau_s}S(t) - k_1S(t) \\ \frac{dT(t)}{dt} &= -\frac{1}{\tau_t}T(t) - k_1T(t) \\ \frac{dG(t)}{dt} &= -\frac{1}{\tau_g}G(t) \\ \frac{dM(t)}{dt} &= k_1(S(t) + T(t)) - k_1M(t) \\ \frac{dX(t)}{dt} &= k_1M(t) - \frac{1}{\tau_x}X(t) \end{aligned} \quad (8)$$

Here, k_1 is the rate at which the excited argon dimers transfer energy to the mixed state, and then to the xenon. This is related to the diffusion in liquid argon.

These equations can be solved analytically. Using MATLAB's symbolic toolkit, we arrive at the solutions:

$$\begin{aligned}
S(t) &= S_0 e^{-t(1/\tau_s+k_1)} \\
T(t) &= T_0 e^{-t(1/\tau_t+k_1)} \\
G(t) &= G_0 e^{-t/\tau_g} \\
M(t) &= k_1 (S_0 \tau_s + T_0 \tau_t) e^{-k_1 t} - k_1 (S(t) \tau_s + T(t) \tau_t) \\
X(t) &= \frac{S_0 \tau_s (\tau_x - \tau_t + k_1 \tau_t \tau_x) + T_0 \tau_t (\tau_x - \tau_t + k_1 \tau_s \tau_x)}{(\tau_x - \tau_t + k_1 \tau_t \tau_x)(\tau_x - \tau_t + k_1 \tau_s \tau_x)(k_1 \tau_x - 1)} k_1^2 \tau_x^2 e^{-t/\tau_x} \\
&\quad + \frac{k_1^2 \tau_s^2 \tau_x}{\tau_x - \tau_s + k_1 \tau_s \tau_x} S(t) + \frac{k_1^2 \tau_t^2 \tau_x}{\tau_x - \tau_t + k_1 \tau_t \tau_x} T(t) \\
&\quad - \frac{k_1^2 \tau_x (S_0 \tau_s + T_0 \tau_t)}{k_1 \tau_x - 1} e^{-k_1 t}
\end{aligned} \tag{9}$$

We take the initial concentrations of the mixed and excited xenon states to be zero, as they are populated through a transfer from the argon. There surely is an initial concentration of excited xenon dimers from the passage of the ionizing particle, however as the concentration of xenon is much less than the argon, and the xenon triplet lifetime is much shorter than that of argon, this is negligible.

The preceding derivation gives us the change in the number of molecules in each state. To have a light output, we take the change in these states through the emission of light. This value, $L(t)$ is given as:

$$L(t) = \frac{1}{\tau_s} S(t) + \frac{1}{\tau_t} T(t) + \frac{1}{\tau_g} G(t) + \frac{1}{\tau_x} X(t) \tag{10}$$

$L(t)$ is then the equation which is fitted to data from a photodetector.

2.2 Fits to BACoN Data

Xenon doping at concentrations of 1, 2, 5, and 10 ppm was done with BACoN. In each concentration, as well as in pure LAr, we take the weighted sum of 10,000 scintillation events. This sum is then normalized such that the number of events from all bins is one. The time of the scintillation event, $t = 0$, in data is set to $\sim 1 \mu s$ as a result of our trigger setting. Then to match the model, we ignore the first 40 bins of data. Additionally, in the experiment, the time resolution of the data acquisition was not adequate to resolve the singlet times; the singlet component of the data is only 2 – 3 bins, which is inadequate to fit an exponential $S(t)$. We then chose to ignore the singlet component in our fits. This is justified as the singlet decay is much shorter than the transfer to xenon, and is therefore negligible in the xenon light output. We then also ignore an additional 2 bins of data to remove the singlet component. Additionally, the PMTs suffer from afterpulsing, most likely due to the leakage of helium in the vacuum tubes. Several sharp peaks are then present at early times but are negligible in the overall fit.

As shown in Equations 9 and 10, the fit parameters are: k_1 the diffusive rate constant, and the initial concentration of triplet states, T_0 and G_0 . We expect the ratio of G_0 and

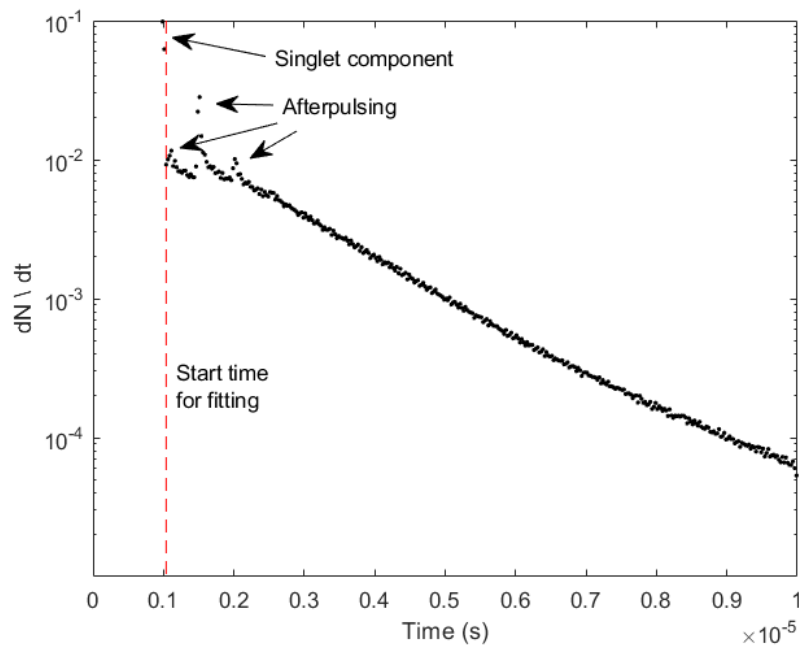


Figure 4: The raw data for the pure LAr. Note that data before the event is noise, and is therefore close to zero and unviewable on a log-scale plot.

T_0 to remain constant, as the ratio of gas to liquid in BACoN is constant. One can then eliminate G_0 as a parameter by fixing the ratio of G_0/T_0 . To do so, we first let both T_0 and G_0 be free parameters in the 10 ppm Xe data set, which has the most pronounced gas component. Doing so, we calculate a ratio of $G_0/T_0 = 0.0585 \pm 0.0028$. In our other fits, we then let $G_0 = 0.0585 T_0$, leaving T_0 free.

With these considerations, we then fit to the data. The results are shown in Figure 6 and Table 1.

Fitting Parameters		
Xe Concentration (ppm)	k_1 (μs^{-1})	T_0
0	0.700 ± 0.016	0.0187 ± 0.0003
1	0.566 ± 0.020	0.0203 ± 0.0018
2	0.939 ± 0.028	0.0201 ± 0.0062
5	1.782 ± 0.025	0.0224 ± 0.0052
10	2.584 ± 0.034	0.0212 ± 0.0036

Table 1: The values for the fitting parameters. Note that the values of T_0 are not the actual concentrations, as the data has been normalized. Additionally, as different amounts of light are produced in each data set, and therefore the normalization is different, one cannot compare T_0 across fits.

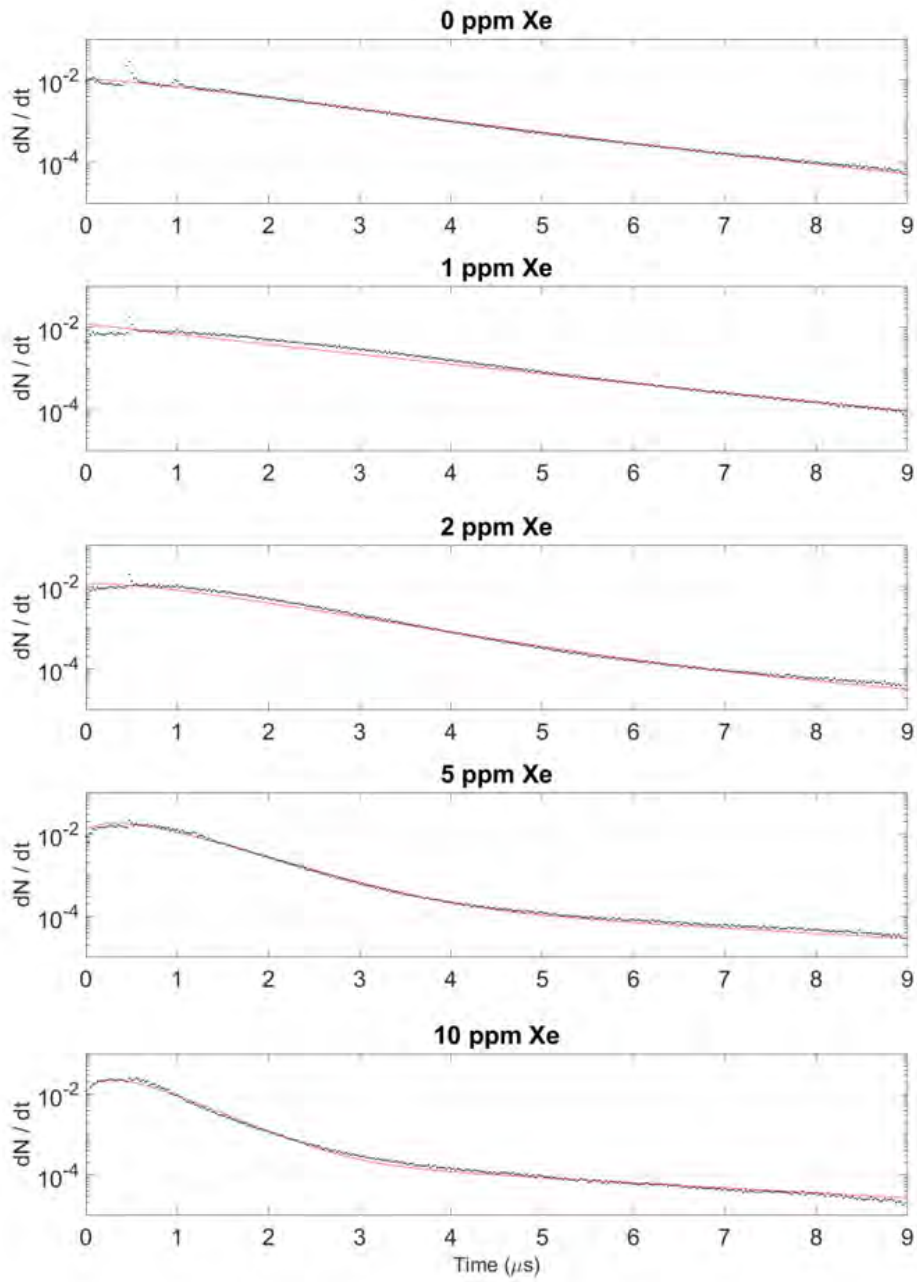


Figure 5: The results of our fits to various xenon concentrations. Note the y-scale is logarithmic. Qualitatively, one can observe the shifting of light to earlier times as the xenon concentration is increased. One can note that at higher concentrations, a long tail emerges, which is the long-lived gaseous argon triplet light.

2.3 Analysis of Rate Constant

The rate constant k_1 is the relevant parameter in this model, quantifying the effects of xenon doping. The transfer from argon to xenon is dictated by diffusion, and k_1 is then a diffusion constant, which should be linear with respect to concentration.

As shown in Figure 6, there is a positive relation with the xenon concentration. Performing a linear fit, we obtain $k_1 = 0.208 \times (\text{ppm}) + 0.567$, in units of μs^{-1} . The non-zero intercept implies a non-zero initial xenon concentration. This is calculated as (2.73 ± 1.38) ppm. This is consistent with previous studies of liquid argon.

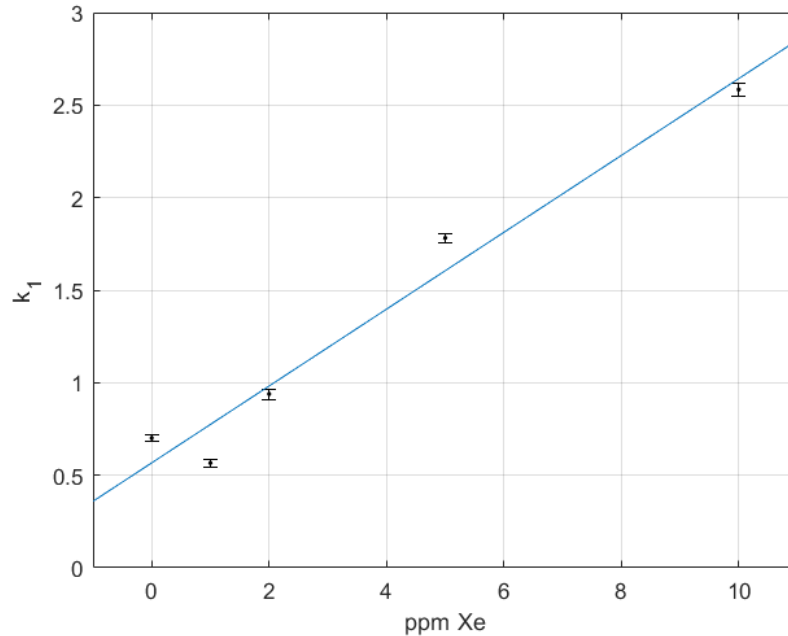


Figure 6: The fitted rate constant k_1 as a function of the xenon concentration. Note that although the 1 ppm fit produces a k_1 lower than the 0 ppm, the 1 ppm fit is poor compared to the others.

3 Instrumentation of SiPMs

Silicon photomultipliers (SiPMs) are solid state devices that are increasingly being used in place of PMTs. SiPMs offer a number of advantages to PMTs, having greater photodetection efficiency in the VUV, being resilient to magnetic fields, required a much lower operating voltage, and being cost-effective [9]. While PMTs do have a larger window and a lower dark rate, overall, SiPMs hold an advantage. Of importance for BACoN is the need for new and more photodetectors. The two current PMTs have aroused a number of issues, including the mentioned afterpulsing, and a tendency to spark while in operation. Additionally, more photodetectors will allow us to add wavelength filters to view only argon or xenon scintillation light.

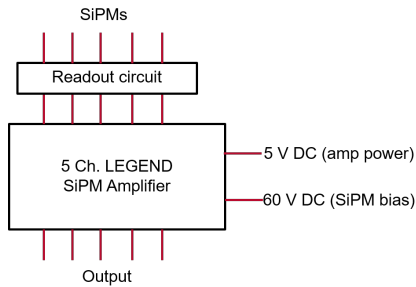


Figure 7: Overview of the SiPM testing setup. The breakdown voltage is 55 V, with an overvoltage of 5 V recommended by the manufacturer.

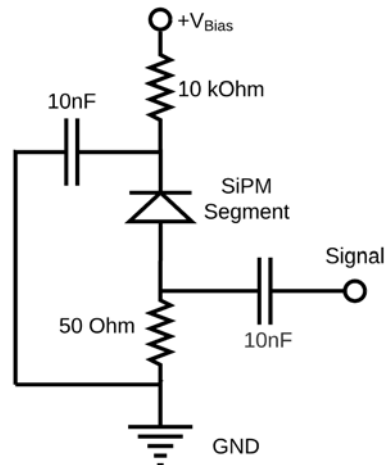


Figure 8: A simplified SiPM readout circuit diagram [9].

We have obtained ten Hamamatsu S13370-3050CN SiPMs. Before installation in BACoN, preliminary testing is needed to determine electronic configurations and develop an analysis protocol. The testing setup is outlined in Figures 7 and 8. We have achieved a definite signal, however, a data set with full analysis is still in progress.

4 Conclusions and Future Work

Xenon doping in liquid argon has been shown to improve the light yield. To fully understand the effects of xenon doping, I present a fitting method of the scintillation light based on a physical model, which is fit to five sets of data from BACoN, a liquid argon test stand. Additionally, for further studies with BACoN, I have taken the first steps towards calibrating silicon photomultipliers.

For future work, we wish to use this model on previous xenon doping studies, which utilize higher concentrations. Furthermore, a global fitting method is desired; that is, a method where parameters are fit from all data sets. Additionally, a full calibration of the silicon photomultipliers and installation in BACoN will be done. Future work with BACoN may include xenon doping at higher concentrations, and testing xenon doped liquid argon with germanium detectors inserted.

Acknowledgements

I am grateful for the financial support from the Rayburn Reaching Up Fund and the New Mexico Space Grant Consortium. I would also like to acknowledge the equipment provided by Los Alamos National Laboratory, the University of Washington, and the University of North Carolina.

I am grateful to my advisor, Michael Gold, whose mentorship and patience guided me

through this work and through my time at UNM. I would also like to thank Doug Fields, who was instrumental in much of my research. Thank you also to Neil McFadden, Dinesh Loomba, and Jim Thomas for their support and assistance.

References

- [1] Bogdan Povh. *Particles and Nuclei: An Introduction to the Physical Concepts*. Springer, 2015.
- [2] Carlo Giunti and Chung W. Kim. *Fundamentals of Neutrino Physics and Astrophysics*. Oxford, 2007.
- [3] Michelle J. Dolinski, Alan W.P. Poon, and Werner Rodejohann. Neutrinoless double-beta decay: Status and prospects. *Annual Review of Nuclear and Particle Science*, 69(1):219–251, Oct 2019.
- [4] Jordan Myslik. Legend: The large enriched germanium experiment for neutrinoless double-beta decay, 2018.
- [5] C.G. Wahl, E.P. Bernard, W.H. Lippincott, J.A. Nikkel, Y. Shin, and D.N. McKinsey. Pulse-shape discrimination and energy resolution of a liquid-argon scintillator with xenon doping. *JINST*, 9:P06013, 2014.
- [6] Michael Akashi-Ronquest, Amanda Bacon, Christopher Benson, Kolahal Bhattacharya, Thomas Caldwell, Joseph A. Formaggio, Dan Gastler, Brianna Grado-White, Jeff Griego, Michael Gold, and et al. Triplet lifetime in gaseous argon. *The European Physical Journal A*, 55(10), Oct 2019.
- [7] R. Acciarri et al. Effects of Nitrogen contamination in liquid Argon. *JINST*, 5:P06003, 2010.
- [8] D. Akimov, V. Belov, A. Konovalov, A. Kumpan, O. Razuvaeva, D. Rudik, and G. Simakov. Fast component re-emission in xe-doped liquid argon. *Journal of Instrumentation*, 14(09):P09022–P09022, Sep 2019.
- [9] Laura Baudis, Michelle Galloway, Alexander Kish, Chris Marentini, and Julien Wulf. Characterisation of Silicon Photomultipliers for Liquid Xenon Detectors. *JINST*, 13(10):P10022, 2018.